

Observation of two output light pulses from a partial wavelength converter preserving phase of an input light at a single-photon level

Rikizo Ikuta,^{1,*} Toshiki Kobayashi,¹ Hiroshi Kato,¹
Shigehito Miki,² Taro Yamashita,² Hirotaka Terai,² Mikio Fujiwara,³
Takashi Yamamoto,¹ Masahide Sasaki,³ Zhen Wang,² Masato Koashi,⁴
and Nobuyuki Imoto¹

¹Graduate School of Engineering Science, Osaka University, Toyonaka, Osaka 560-8531, Japan

²Advanced ICT Research Institute, National Institute of Information and Communications Technology (NICT), Kobe 651-2492, Japan

³Advanced ICT Research Institute, National Institute of Information and Communications Technology (NICT), Koganei, Tokyo 184-8795, Japan

⁴Photon Science Center, The University of Tokyo, Bunkyo-ku, Tokyo 113-8656, Japan

[*rikuta@mp.es.osaka-u.ac.jp](mailto:rikuta@mp.es.osaka-u.ac.jp)

Abstract: We experimentally demonstrate that both of the two output light pulses of different wavelengths from a wavelength converter with various branching ratios preserve phase information of an input light at a single-photon level. In our experiment, we converted temporally-separated two coherent light pulses with average photon numbers of ~ 0.1 at 780 nm to light pulses at 1522 nm by using difference-frequency generation in a periodically-poled lithium niobate waveguide. We observed an interference between temporally-separated two modes for both the converted and the unconverted light pulses at various values of the conversion efficiency. We observed interference visibilities greater than 0.88 without suppressing the background noises for any value of the conversion efficiency the wavelength converter achieves. At a conversion efficiency of ~ 0.5 , the observed visibilities are 0.98 for the unconverted light and 0.99 for the converted light. Such a phase-preserving wavelength converter with high visibilities will be useful for manipulating quantum states encoded in the frequency degrees of freedom.

© 2018 Optical Society of America

OCIS codes: (270.5565) Quantum communications; (270.5585) Quantum information and processing; (270.1670) Coherent optical effects; (130.7405) Wavelength conversion devices; (190.4223) Nonlinear wave mixing.

References and links

1. P. Kumar, "Quantum frequency conversion," *Opt. Lett.* **15**, 1476–1478 (1990).
2. C. Langrock, E. Diamanti, R. V. Roussev, Y. Yamamoto, M. M. Fejer, and H. Takesue, "Highly efficient single-photon detection at communication wavelengths by use of upconversion in reverse-proton-exchanged periodically poled LiNbO₃ waveguides," *Opt. Lett.* **30**, 1725–1727 (2005).
3. M. T. Rakher, L. Ma, O. Slattery, X. Tang, and K. Srinivasan, "Quantum transduction of telecommunications-band single photons from a quantum dot by frequency upconversion," *Nat. Photonics* **4**, 786–791 (2010).

4. H. Takesue, "Erasing Distinguishability Using Quantum Frequency Up-Conversion," *Phys. Rev. Lett.* **101**, 173901 (2008).
5. S. Tanzilli, W. Tittel, M. Halder, O. Alibart, P. Baldi, N. Gisin, and H. Zbinden, "A photonic quantum information interface," *Nature* **437**, 116–120 (2005).
6. Y. Dudin, A. Radnaev, R. Zhao, J. Blumoff, T. Kennedy, and A. Kuzmich, "Entanglement of Light-Shift Compensated Atomic Spin Waves with Telecom Light," *Phys. Rev. Lett.* **105**, 260502 (2010).
7. R. Ikuta, Y. Kusaka, T. Kitano, H. Kato, T. Yamamoto, M. Koashi, and N. Imoto, "Wide-band quantum interface for visible-to-telecommunication wavelength conversion," *Nat. Commun.* **2**, 1544 (2011).
8. S. Zaske, A. Lenhard, C. Keßler, J. Kettler, C. Hepp, C. Arend, R. Albrecht, W.-M. Schulz, M. Jetter, P. Michler, and C. Becher, "Visible-to-Telecom Quantum Frequency Conversion of Light from a Single Quantum Emitter," *Phys. Rev. Lett.* **109**, 147404 (2012).
9. R. Ikuta, H. Kato, Y. Kusaka, S. Miki, T. Yamashita, H. Terai, M. Fujiwara, T. Yamamoto, M. Koashi, M. Sasaki, Z. Wang, and N. Imoto, "High-fidelity conversion of photonic quantum information to telecommunication wavelength with superconducting single-photon detectors," *Phys. Rev. A* **87**, 010301 (2013).
10. R. Ikuta, T. Kobayashi, H. Kato, S. Miki, T. Yamashita, H. Terai, M. Fujiwara, T. Yamamoto, M. Koashi, M. Sasaki, Z. Wang, and N. Imoto, "Nonclassical two-photon interference between independent telecommunication light pulses converted by difference-frequency generation," *Phys. Rev. A* **88**, 042317 (2013).
11. M. Raymer, S. van Enk, C. McKinstrie, and H. McGuinness, "Interference of two photons of different color," *Opt. Commun.* **283**, 747–752 (2010).
12. H. Takesue, "Single-photon frequency down-conversion experiment," *Phys. Rev. A* **82**, 013833 (2010).
13. N. Curtz, R. Thew, C. Simon, N. Gisin, and H. Zbinden, "Coherent frequency-down-conversion interface for quantum repeaters," *Opt. Express* **18**, 22099–22104 (2010).
14. S. Ramelow, a. Fedrizzi, a. Poppe, N. Langford, and a. Zeilinger, "Polarization-entanglement-conserving frequency conversion of photons," *Phys. Rev. A* **85**, 013845 (2012).
15. G. Giorgi, P. Mataloni, and F. De Martini, "Frequency hopping in quantum interferometry: Efficient up-down conversion for qubits and ebits," *Phys. Rev. Lett.* **90**, 027902 (2003).
16. S. Zaske, A. Lenhard, and C. Becher, "Efficient frequency downconversion at the single photon level from the red spectral range to the telecommunications C-band," *Opt. Express* **19**, 12825–12836 (2011).
17. L. Ma, O. Slattery, and X. Tang, "Single photon frequency up-conversion and its applications," *Phys. Reports* **521**, 69–94 (2012).
18. T. Nishikawa, A. Ozawa, Y. Nishida, M. Asobe, F.-L. Hong, and T. W. Hänsch, "Efficient 494 mW sum-frequency generation of sodium resonance radiation at 589 nm by using a periodically poled Zn:LiNbO₃ ridge waveguide," *Opt. Express* **17**, 17792–17800 (2009).
19. S. Miki, M. Takeda, M. Fujiwara, M. Sasaki, and Z. Wang, "Compactly packaged superconducting nanowire single-photon detector with an optical cavity for multichannel system," *Opt. Express* **17**, 23557–23564 (2009).
20. S. Miki, T. Yamashita, M. Fujiwara, M. Sasaki, and Z. Wang, "Multichannel SNSPD system with high detection efficiency at telecommunication wavelength," *Opt. Lett.* **35**, 2133–2135 (2010).
21. J. S. Pelc, L. Ma, C. R. Phillips, Q. Zhang, C. Langrock, O. Slattery, X. Tang, and M. M. Fejer, "Long-wavelength-pumped upconversion single-photon detector at 1550 nm : performance and noise analysis," *Opt. Express* **19**, 21445–21456 (2011).

1. Introduction

A photonic quantum interface for a wavelength conversion was proposed in 1990 [1], and it has been widely studied for quantum-information applications such as an efficient up-conversion detector [2, 3], a frequency-domain quantum eraser [4], and wavelength conversion aiming at long-distance quantum communication based on quantum repeaters [5–10]. The wavelength conversion between two optical fields through a nonlinear optical medium with a sufficiently strong pump light is described by an effective Hamiltonian of a beamsplitter (BS) in a frequency domain [11]. The wavelength conversion described by such a Hamiltonian is expected to have properties that phases of the converted and the unconverted light pulses take over from the phase of the input light, and that the conversion efficiency is tunable by changing the pump power. In some of the previous demonstrations, it was observed that the converted light preserved the phase of the input light by using a weak coherent light at a single-photon level [12, 13] and by using entangled photons [5–7, 14]. On the other hand, to our best knowledge, none of demonstrations observes that an unconverted light retains phase information of an input light except the work of Giorgi *et al.* [15] in which they observed the phase preservation of converted and unconverted light pulses with interference visibilities of ~ 0.5 and ~ 0.7 , respectively,

at a conversion efficiency of ~ 0.4 . When the conversion efficiency increases, the signal-to-noise ratio of the unconverted mode decreases because the strong pump light increases the optical noises through the conversion process [16, 17] while the light in the unconverted mode decreases. When the conversion efficiency approaches unity, the signal-to-noise ratio will be almost zero. Moreover, in reality the conversion efficiency saturates at a level below unity, which cannot be explained by the simple Hamiltonian. Therefore, it is not obvious that the unconverted light holds phase information of the input light for high conversion efficiencies, and it is worth observing the phase preservation of not only the converted light but also the unconverted light for evaluating the basic property of the wavelength conversion working in a quantum regime.

In this paper, we demonstrate that two output light pulses of different wavelengths after wavelength conversion inherit phase information of the input light with high visibilities. Observed interference visibilities are over 0.88 without suppressing the background noises regardless of the conversion efficiencies our wavelength converter achieves. At a conversion efficiency of ~ 0.5 , the observed visibilities are 0.98 for the unconverted light and 0.99 for the converted light. The wavelength conversion is achieved by the difference-frequency generation (DFG) in a periodically-poled lithium niobate (PPLN) waveguide. We used temporally-separated two light pulses at a single-photon level from a laser source at 780 nm as the input. The wavelength of the photons is converted to 1522 nm with various conversion efficiencies by choosing the pump power at 1600 nm. We observed an interference between temporally-separated two modes for both the converted and the unconverted light pulses. The operation of the partial wavelength converter which splits an input light into two different wavelengths while preserving the phase information is similar to the conventional beamsplitter dividing the input into two spatial modes. Therefore such a wavelength converter will be useful for manipulating quantum states encoded in the frequency degrees of freedom.

2. Theory of an ideal wavelength conversion

We summarize the quantum dynamics of an ideal wavelength conversion based on difference frequency generation (DFG) in a nonlinear optical medium as follows [1, 7]. We suppose that a signal mode at angular frequency ω_s and a converted mode at angular frequency ω_c satisfies $\omega_c = \omega_s - \omega_p$, where ω_p is the angular frequency of the pump light. When the pump light is sufficiently strong, the effective Hamiltonian of the DFG process is described by

$$\hat{H} = i\hbar(\xi^* \hat{a}_c^\dagger \hat{a}_s - \xi \hat{a}_s^\dagger \hat{a}_c), \quad (1)$$

where \hat{a}_s and \hat{a}_c are annihilation operators of the signal mode and the converted mode, respectively. Here $\xi = |\xi|e^{i\phi}$ is proportional to the complex amplitude of the classical pump light. By using Eq. (1), annihilation operators $\hat{a}_{s,\text{out}}$ and $\hat{a}_{c,\text{out}}$ of the signal and converted modes from the nonlinear optical medium are described by

$$\hat{a}_{c,\text{out}} = e^{-i\phi} \sin(|\xi|\tau) \hat{a}_s + \cos(|\xi|\tau) \hat{a}_c \quad (2)$$

and

$$\hat{a}_{s,\text{out}} = \cos(|\xi|\tau) \hat{a}_s - e^{i\phi} \sin(|\xi|\tau) \hat{a}_c, \quad (3)$$

where τ is the propagation time of the pulses through the nonlinear optical medium. Eqs. (2) and (3) are equivalent to the relation between input and output modes of a BS. The transmittance and the reflectance are $|\cos(\xi\tau)|^2$ and $|\sin(\xi\tau)|^2$, respectively. These can be adjusted by changing the pump power for the wavelength conversion. From Eqs. (2) and (3), the converted light and the remaining unconverted light take over the phase information from the input signal light. In

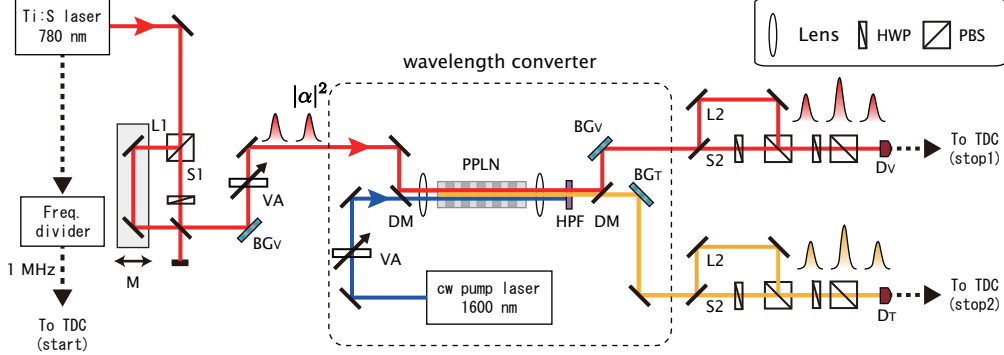


Fig. 1. Experimental setup. We initially prepare two temporally-separated light pulses at 780 nm. Their frequencies are down-converted to 1522 nm by DFG in the PPLN. The length of the PPLN crystal is 20 mm, and the acceptable bandwidth is calculated to be 0.3 nm. The conversion efficiency is changed by the pump power up to ~ 700 mW. After the process of the wavelength conversion, the interference fringe of each of the unconverted light at 780 nm and the converted light at 1522 nm is measured.

the experiments in [5–7, 12–14], the phase preservation of the converted light in Eq. (2) has been demonstrated. On the other hand, that of the unconverted light in Eq. (3) has not been observed with a high fidelity [15].

3. Experiment

3.1. Experimental setup

The experimental setup is shown in Fig. 1. We use a $+45^\circ$ polarized mode-locked Ti:sapphire (Ti:S) laser (wavelength: 780 nm; pulse width: 1.2 ps; repetition rate: 82 MHz) as a light source. The light is divided into a short path (S1) and a long path (L1) by a polarizing beamsplitter (PBS). After the polarization of the light passing through S1 is flipped from horizontal (H) to vertical (V) polarization by a half wave plate (HWP), they are recombined by a BS. The time difference of about 600 ps gives phase difference between the two light pulses, and it is varied by mirrors (M) on a piezo motor driven stage. After the light pulses are spectrally narrowed by a Bragg grating (BG_V) with a bandwidth of 0.2 nm, an average photon number of each of the temporally-separated light pulses is set to $|\alpha|^2$, which can be varied from 10^{-3} to 1 by a variable attenuator (VA). Then the light pulses are coupled to the quasi-phase-matched PPLN waveguide [18]. Their frequencies are down-converted to the wavelength of 1522 nm by the DFG using a cw pump laser at 1600 nm which is combined with the signal light by a dichroic mirror (DM). The conversion efficiency is changed by the pump power up to ~ 700 mW.

After the wavelength conversion, the pump light is eliminated by a high-pass filter (HPF), and the light pulses at 780 nm and 1522 nm are separated by a DM. The temporally-separated light pulses at 780 nm are diffracted by another BG_V , while the light pulses at 1522 nm are diffracted by BG_T with a bandwidth of 1 nm. The temporally-separated two light pulses at each wavelength are divided into a short path (S2) and a long path (L2) with a time difference of 600 ps. After the polarization of the light passing through S2 is flipped, the light pulses from S2 and L2 are mixed by a PBS. Finally, the light pulses are projected onto $+45^\circ$ polarization, and then coupled to single-mode fibers followed by superconducting single-photon detectors (SSPDs) [19, 20] which are denoted by D_V for the light at 780 nm and D_T for the light

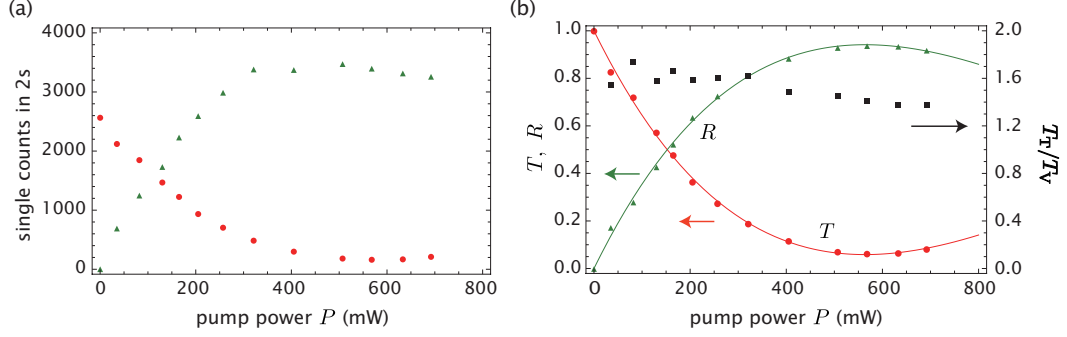


Fig. 2. (a) Observed counts of the unconverted photons (red circle) and the converted photons (green triangle). (b) The probability of the unconverted events T (red circle), the conversion efficiency $R = 1 - T$ (green triangle) and the ratio of T_T to T_V (black square). We derived the curve for $T(P)$ by using the observed photon counts of the unconverted light. The red curve for T is obtained by the best fit to T with $1 - A \sin^2(\sqrt{\eta P})$, where $A \approx 0.94$ and $\eta \approx 0.0044/\text{mW}$. The green curve for R is given by $A \sin^2(\sqrt{\eta P})$.

at 1522 nm.

Electric signals from D_V and D_T are connected to a time-to-digital converter (TDC) which is gated by a 1-MHz clock signal. The clock signal is obtained by frequency division of the 82 MHz clock signal from Ti:S laser. There are three possible arrival times in the electric signals from D_V and D_T . The earliest and the latest signals are obtained by the light passing through S1-S2 and L1-L2 paths, respectively. We post-select the 200-ps time windows of the central peaks originated with the light pulses passing through S1-L2 and L1-S2. Such post-selected signals from D_V and D_T should show the first-order interference pattern of the coherent light pulses at 780 nm and 1522 nm, respectively, depending on the position of M.

3.2. Experimental results

Before we describe the demonstration of the phase-preservation property of our wavelength converter, we first observed the dependencies of the probability of the unconverted events and the conversion efficiency on the pump power by measuring the photon counts of the unconverted mode at 780 nm and the converted mode at 1522 nm. In this experiment, we set $|\alpha|^2$ to ~ 0.1 . The experimental result is shown in Fig. 2(a). From the result, the maximum conversion efficiency is achieved at the pump power of ≈ 560 mW which is smaller than the maximum pump power of 700 mW we can supply. We roughly estimate the internal conversion efficiency in the PPLN crystal as follows. The transmittance of the optical circuit before the wavelength conversion including the coupling efficiency to the PPLN is represented by T_{in} . The conversion efficiency and the probability of the unconverted events are represented by $R(P)$ and $1 - R(P) = T(P)$, respectively, where P is the pump power. Note that $R(P)$ corresponds to $|\sin(\xi \tau)|^2$ in Eqs. (2) and (3). We denote overall transmittance of the optical circuit including the quantum efficiency of the detector after the conversion process by T_V for the unconverted light at 780 nm. The detection counts of the unconverted light pulse is described by $C = \mathcal{N} T_{\text{in}} T(P) T_V$, where \mathcal{N} is the total number of the input photons. We assume that T_{in} and T_V take constant values regardless of the pump power. By using $T(0 \text{ mW}) = 1$ and the observed count of $C_0 = \mathcal{N} T_{\text{in}} T_V$ at $P = 0$ mW, we obtain the dependency of $C/C_0 = T(P)$ on the pump power as shown in Fig. 2(b). The best fit to $T(P)$ with $1 - A \sin^2(\sqrt{\eta P})$ gives $A \approx 0.94$ and $\eta \approx 0.0044/\text{mW}$.

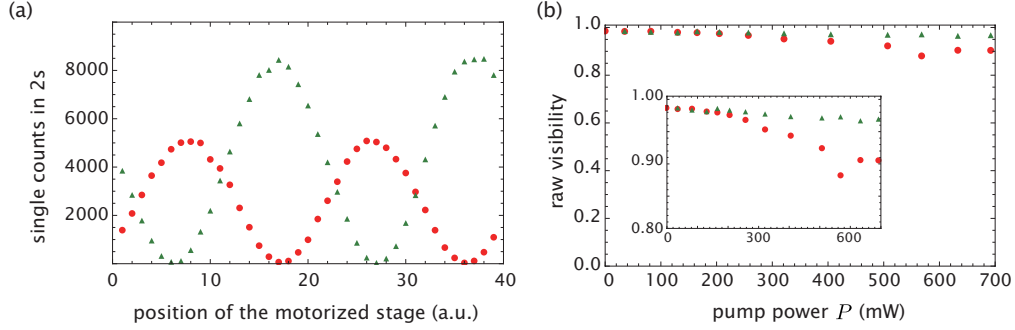


Fig. 3. (a) The interference fringes of the unconverted photons (red circle) and the converted photons (green triangle). These data were observed at the pump power of 165 mW, namely $T \approx 0.5$. The interference visibilities are 0.98 for the unconverted light and 0.99 for the converted light. (b) Dependencies of the visibilities on the pump power. The inset shows the enlarged view.

When we denote overall transmittance after the conversion process by T_T for the converted light at 1522 nm, the detection counts of the converted light is given by $\mathcal{N}T_{\text{in}}R(P)T_T$. Because $\mathcal{N}T_{\text{in}}R(P)T_T/C_0 = R(P)T_T/T_V$ and $R(P) = 1 - T(P)$, T_T/T_V is estimated from the observed photon count of the unconverted light and that of the converted light at each pump power, which is shown in Fig. 2(b). We see that T_T/T_V takes an almost constant value of about 1.5, which is in accord with the assumption of T_V being constant in our rough estimation.

Next we demonstrated that both the unconverted and the converted light pulses after the wavelength conversion preserve the phase information of the input light pulse. In this demonstration, the average photon number of the input light was set to $|\alpha|^2 \approx 0.1$. By moving mirror M in Fig. 1, the time difference between the light pulses passing through S1 and L1 is varied. As a result, the first-order interference fringe is observed after mixing the light pulses passing through the paths of S1-L2 and L1-S2. Fig. 3(a) shows the experimental result of the interference fringe when the pump power is 165 mW. For both the unconverted and the converted light pulses, the interference fringes are clearly observed. We define the interference visibility by $V = (N_{\text{max}} - N_{\text{min}})/(N_{\text{max}} + N_{\text{min}})$, where N_{max} and N_{min} are the maximum and the minimum of the count rates, respectively. The observed values of the visibilities are $V = 0.98$ for the unconverted light and $V = 0.99$ for the converted light. The standard deviations of the visibilities with the assumption of the Poisson statistics of the counts are less than 0.01. We then measured the visibilities of the interference for various values of the pump power ranging from 0 mW to 700 mW. The experimental results are shown in Fig. 3(b). For both the converted and the unconverted light pulses, we observed visibilities higher than 0.88.

From the experimental result in Fig. 3(b), we see that the visibilities decrease with the pump power more prominently for the unconverted mode. In order to see the reason for the degradation of the visibilities, we measured the background noises from the detected counts temporally away from the three signal peaks. The average noise counts are shown in Fig. 4(a). For the converted mode at 1522 nm, the linear dependency of the noise photons on the pump power is observed, which is caused by the Raman scattering of the pump light for the DFG [7, 16]. On the other hand, for the unconverted mode at 780 nm, nonlinear dependency of the noise photons on the pump power is observed. Such a dependency has been reported in a lot of demonstrations of frequency up-conversion to a visible light [2, 17, 21]. They claim that when we use a pump light longer than a signal light and a converted light, the optical noises are mainly originated

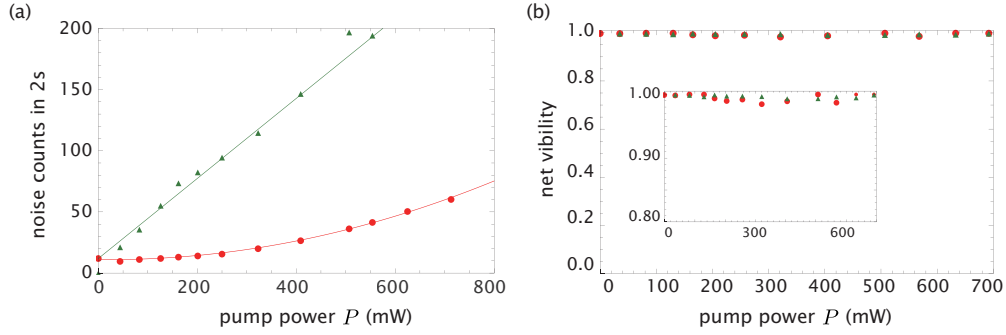


Fig. 4. (a) Dependencies of the background noises on the pump power. The green triangles show the result for the unconverted visible photons. The red circles show the result for the converted telecom photons. The background noise of the unconverted mode when the pump light is off is slightly larger than zero while the dark count of the detector D_V is almost zero, indicating that such a noise may be caused by a component of the residual fundamental cw light as a result of the imperfection of the signal light from the Ti:S laser. (b) Dependencies of the net visibilities on the pump power. The green triangles and the red circles show the results for the unconverted visible and the converted telecom photons, respectively.

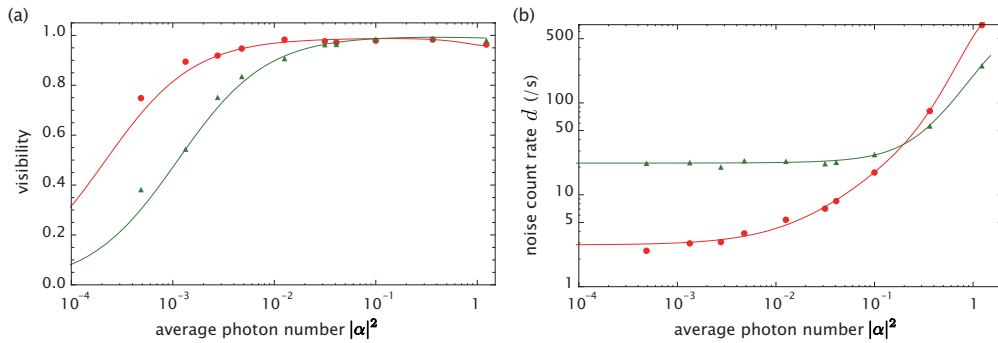


Fig. 5. (a) Dependencies of the visibilities on $|\alpha|^2$ when the pump power is 165 mW. The points of the red circle and the green triangle show the visibilities of the unconverted photons and the converted photons, respectively. The solid curves are obtained by using the signal-photon rates estimated from the experimental data and the observed noise counts shown in Fig. 5(b). (b) Dependencies of the noise counts on $|\alpha|^2$. The points of the red circle and the green triangle are for the unconverted photons and the converted photons, respectively. The solid curves are obtained by using polynomial functions fitted to the observed noise count rate d .

from the Raman scattering of the pump light followed by its frequency up-conversion. By subtracting the background noises, we plotted the net visibilities in Fig. 4(b). The net visibilities exceed 0.98 for all pump powers. The result indicates that the degradation of the visibilities are mainly caused by the optical noises from the pump light.

Finally, we measured the interference visibility for various values of $|\alpha|^2$ with the fixed pump power of 165 mW. The observed values of V are shown in Fig. 5(a). The high visibilities over 0.9 remain for the converted and the unconverted light pulses for $|\alpha|^2 > 0.01$. The behavior of the visibilities in Fig. 5(a) can be explained by using temporally continuous background noises

depending on $|\alpha|^2$, which was separately measured and is shown in Fig. 5(b). We assume the noise photons are statistically independent of the signal photon counts. Due to the estimated values of the visibilities close to 1 when we subtracted the background noises from the experimental result in Fig. 4(b), we construct a simple model of the visibilities described by the signal photons with unit visibility and the noise photons. In this model, the visibility is given by $V = |\alpha|^2 T_{\text{all}} f / (|\alpha|^2 T_{\text{all}} f + 2d)$, where T_{all} is the overall transmittance of the optical circuit described by $T_{\text{in}} T(P) T_{\text{V}}$ for the unconverted mode and by $T_{\text{in}} R(P) T_{\text{T}}$ for the converted mode. We roughly estimate $T_{\text{in}} T_{\text{V}} \approx 0.03$ for the unconverted mode and $T_{\text{in}} T_{\text{T}} \approx 0.04$ for the converted mode from the observed values. From Fig. 2(b), we see $R(165 \text{ mW}) = T(165 \text{ mW}) = 0.5$. $f = 1$ MHz is the frequency of the clock and d is the rate of the noise photons. By using polynomial functions fitted to the experimental result of the rates of the noise photons for d as shown in Fig. 5(b), we obtain the expected curves of the visibilities shown in Fig. 5(a), which are in good agreement with the experimental data. From the high visibilities for $|\alpha|^2$ much smaller than 1, the phase-preserving property of the wavelength converter will be expected to hold in a quantum regime. We note that the noise-photon rates take almost constant values for $|\alpha|^2 < 0.01$. These values are the intrinsic optical noises generated through the DFG. On the other hand, for larger values of $|\alpha|^2$, the noise-count rates increase. We guess this increase may come from the imperfection in the signal light from the Ti:S laser. Because the residual fundamental cw component of the laser is frequency-converted continuously, the effect of the cw component contributes to the constant background photon counts.

4. Conclusion

In conclusion, we have demonstrated that the two output pulses at different wavelengths from the DFG-based wavelength converter using the PPLN crystal keep the phase information of the input light with high visibilities. By using the temporally-separated two coherent light pulses at 780 nm with average photon numbers smaller than 1 as the input light pulse, we observed the interference between temporally-separated two modes for both the converted and the unconverted light pulses after the wavelength conversion. The observed values of the visibility are over 0.88 for all conversion efficiencies achievable with our wavelength converter. At a conversion efficiency of ~ 0.5 , the observed visibilities are 0.98 for the unconverted light and 0.99 for the converted light.

Acknowledgments

This work was supported by the Funding Program for World-Leading Innovative R & D on Science and Technology (FIRST), MEXT Grant-in-Aid for Scientific Research on Innovative Areas 21102008, MEXT Grant-in-Aid for Young scientists(A) 23684035, JSPS Grant-in-Aid for Scientific Research(A) 25247068 and (B) 25286077.